

**EXTENDED NON-THERMAL EMISSION POSSIBLY ASSOCIATED WITH
CYG OB2 #5**Gisela N. Ortiz-León¹, Luis F. Rodríguez^{1,2} and Mauricio Tapia³

RESUMEN

Cyg OB2 #5 es un sistema binario de contacto (O6.5-7+O5.5-6) con emisión de radio asociada. Dos fuentes compactas ($\leq 0''.3$) de radiocontinuo han sido reportadas anteriormente: la primaria está asociada con la binaria de contacto y la secundaria es una fuente con forma de arco proyectada a $\sim 0''.8$ al NE de la primaria. Esta fuente con forma de arco resulta de la interacción de los vientos de la binaria de contacto y de una estrella tipo B en la región. En este artículo reportamos la detección de una componente extendida ($\sim 30''$) y no-térmica al NE de las componentes compactas. Proponemos que esta emisión extendida podría ser una fuente de fondo (i. e. una radiogalaxia), emisión galáctica extendida, o emisión no-térmica relacionada con electrones relativistas que se producen en el choque entre la binaria de contacto y la estrella tipo B y que son arrastrados a grandes distancias por el viento de la binaria de contacto.

ABSTRACT

Cyg OB2 #5 is a contact binary system (O6.5-7+O5.5-6) with associated radio continuum emission. Two compact ($\leq 0''.3$) radio continuum components have been reported previously: the primary one is associated with the contact binary and the secondary one is an arc-like source $\sim 0''.8$ to the NE of the primary. This arc-like source results from the interaction of the winds of the contact binary and a B-type star in the region. In this paper we report the detection of an extended ($\sim 30''$), non-thermal component to the NE of the compact components. We propose that this extended emission could be an unresolved background source (i. e. a radio galaxy), extended galactic emission, or non-thermal emission related with relativistic electrons that are produced in the shock between the contact binary and the B-type star and that are carried away to large distances by the wind from the contact binary.

Key Words: STARS: INDIVIDUAL (CYG OB2 #5) — RADIO CONTINUUM: STARS

1. INTRODUCTION

Cyg OB2 #5 (V729 Cyg, BD +40 4220) is an eclipsing, contact binary system (apparent spectral types O6.5-7+O5.5-6; Rauw et al. 1999) with a 6.6-day orbital period (Hall 1974; Leung & Schneider 1978; Linder et al. 2009). As several other luminous O-star systems in the Cyg OB2 association, this source is known to have associated variable radio emission (e.g. Persi et al. 1985, 1990; Bieging et al. 1989). In addition to the radio emission coincident with the contact binary, Abbott et al. (1981) and Miralles et al. (1994) reported on the existence of a radio “companion” $0''.8$ to the NE of the contact binary. Observations by Contreras et al. (1997) revealed that this radio source has an elongated shape and lies in-between the contact binary and a third star, which was first reported by Herbig (1967). Contreras et al. (1997) suggested that the proposed NE radio “companion” actually corresponds to the wind interaction zone between the binary system and the

¹Centro de Radioastronomía y Astrofísica, Universidad Nacional Autónoma de México, Campus Morelia

²Astronomy Department, Faculty of Science, King Abdulaziz University, P.O. Box 80203, Jeddah 21589, Saudi Arabia

³Instituto de Astronomía, Universidad Nacional Autónoma de México, Ensenada

tertiary component. Recently, Kennedy et al. (2010) reanalyzed all VLA observations of Cyg OB2 #5 and showed that the primary radio source, associated with the eclipsing binary, varies with a period of 6.7 ± 0.2 yr while the flux from the secondary NE source remains constant in time. It is now known that the variable radio emission closely associated with the eclipsing binary comes from a ~ 10 milliarcsecond arc-shaped source that traces the wind-collision region between the strong wind driven by the contact binary and that of an unseen companion (Ortiz-León et al. 2011).

TABLE 1
VLA ARCHIVE DATA USED (PROJECT AR110)

| Epoch | 6-cm | | | Time on Source (min) | Flux of 2007+404 ^a (Jy) |
|-------------|-------------------------|--|-----------------------------------|-------------------------|--|
| | Time on Source (min) | Flux of 2007+404 ^a (Jy) | Beam Angular Size ^b | | |
| 1984 Sep 06 | 30.5 | 4.415±0.009 | 14''82 × 13''15; +47.0° | 31.0 | 3.977±0.022 |
| 1984 Sep 15 | 31.7 | 4.119±0.089 | 13''22 × 12''16; -49.2° | 41.7 | 3.618±0.114 |
| 1984 Sep 20 | 32.6 | 4.347±0.006 | 15''01 × 13''52; +64.5° | 31.8 | 4.011±0.051 |
| 1984 Sep 22 | 17.5 | 4.151±0.015 | 13''92 × 12''43; +51.7° | 17.0 | 3.856±0.052 |
| 1984 Sep 24 | 45.5 | 4.372±0.016 | 14''22 × 12''81; -70.2° | 45.0 | 4.132±0.025 |
| 1984 Sep 28 | 40.0 | 4.211±0.009 | 13''28 × 12''33; -0.71° | 40.5 | 4.015±0.033 |

^aThe phase calibrator for all the observations was 2007+404.

^bMajor axis × minor axis; position angle, for a (u,v) weighting of ROBUST = 0 (Briggs 1995).

As part of a VLA archive analysis of this source, we concatenated 6 and 20-cm data obtained in the compact configuration D in six epochs during September of 1984. These deep images reveal the presence of an extended emission component apparently associated with Cyg OB2 #5 whose characteristics and possible nature are discussed here.

2. DATA REDUCTION

The archive data from the Very Large Array (VLA) of the NRAO⁴ were edited and calibrated using the software package Astronomical Image Processing System (AIPS) of NRAO. The parameters of the observations are given in Table 1. The absolute amplitude calibrator for five of the six epochs was 1331+305, with an adopted flux density of 7.49 Jy at 6 cm and 14.39 Jy at 20 cm. The amplitude calibrator for 1984 September 22 was 0137+331, with an adopted flux density of 5.43 Jy at 6 cm and 15.29 Jy at 20 cm. The phase calibrator was 2007+404 for all six epochs, with the bootstrapped flux densities given in Table 1.

An image of the 6 cm emission made with the ROBUST parameter of AIPS set equal to 0 is shown in the top part of Figure 1. This image was made using only baselines longer than 1 kλ to suppress structures larger than $\sim 3'.4$. The image shows a bright source at the center. This emission is the spatially unresolved combination of the emission from the contact binary and the NE component. In addition to this bright source there is an extended, faint component to the NE. This component is not reported previously, most probably because for the VLA configurations A and B, structures as large as this component are resolved out. At C and D configurations, the archive data analyzed by us is much better and sensitive than other databases available. We discuss its possible nature in what follows.

The 6 cm and 20 cm data were self-calibrated in phase using all the positive clean components of the sources in the field shown in Figure 2 to model the emission. In this Figure we show a larger part of the same image, where it can be appreciated that the only significant features (above 4-sigma) are Cyg OB2 #5, the extension to the NE and several compact sources in the region. In this same Figure we show a 20 cm image of the same region. To obtain a reliable comparison, both the 6 and 20-cm data were restricted to baselines larger than

⁴The National Radio Astronomy Observatory is operated by Associated Universities Inc. under cooperative agreement with the National Science Foundation.

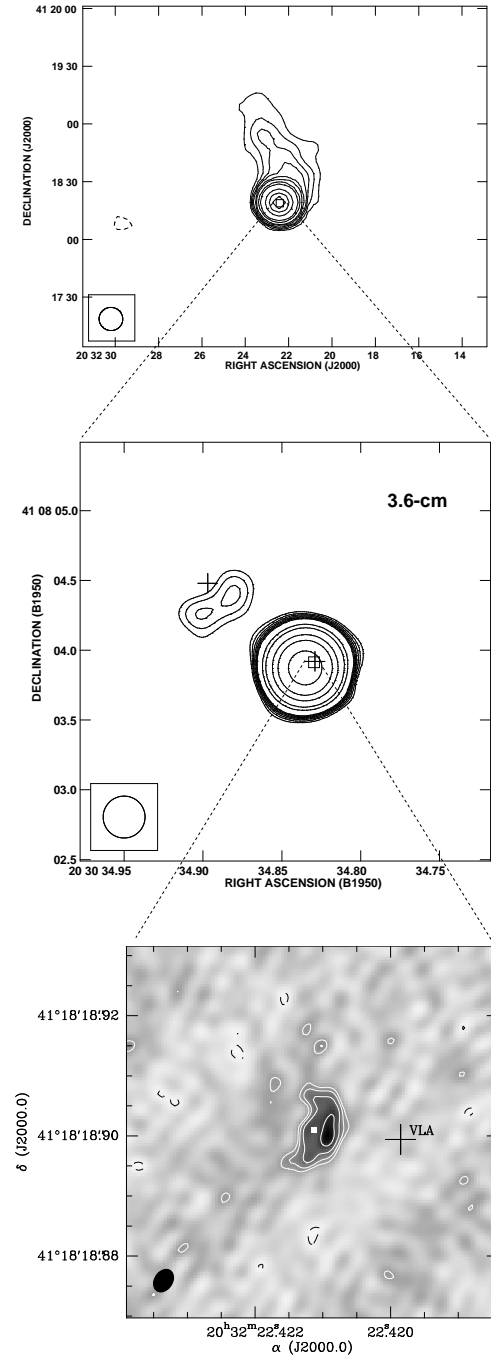


Fig. 1. (Top) VLA contour image of the 6-cm continuum emission toward Cyg OB2 #5. Contours are -3, 3, 4, 5, 6, 8, 10, 15, 20, 40, 60 and 80 times $79 \mu\text{Jy}$, the rms noise of the image. The synthesized beam, shown in the bottom left corner, has half power full width dimensions of $12''.3 \times 12''.0$, with the major axis at a position angle of $+13^\circ$. The bright source at the center coincides with Cyg OB2 #5 and comprises the emission from the contact binary and the compact NE component. The extended emission to the NE is first reported here. (Middle) High-angular resolution 3.6-cm emission from Cyg OB2 #5, from Contreras et al. (1997). The source at the center is the emission from the contact binary and that to the NE corresponds to the compact NE component. The crosses mark the position of the contact binary (center) and of the known B-type star to the NE (Herbig 1967). (Bottom) VLBA image at 3.6 cm from Ortiz-León et al. (2011). The arc-shaped source traces the wind-collision region between the wind of the contact binary (whose position is indicated with a cross) and the undetected companion (whose estimated position is indicated with a white square).

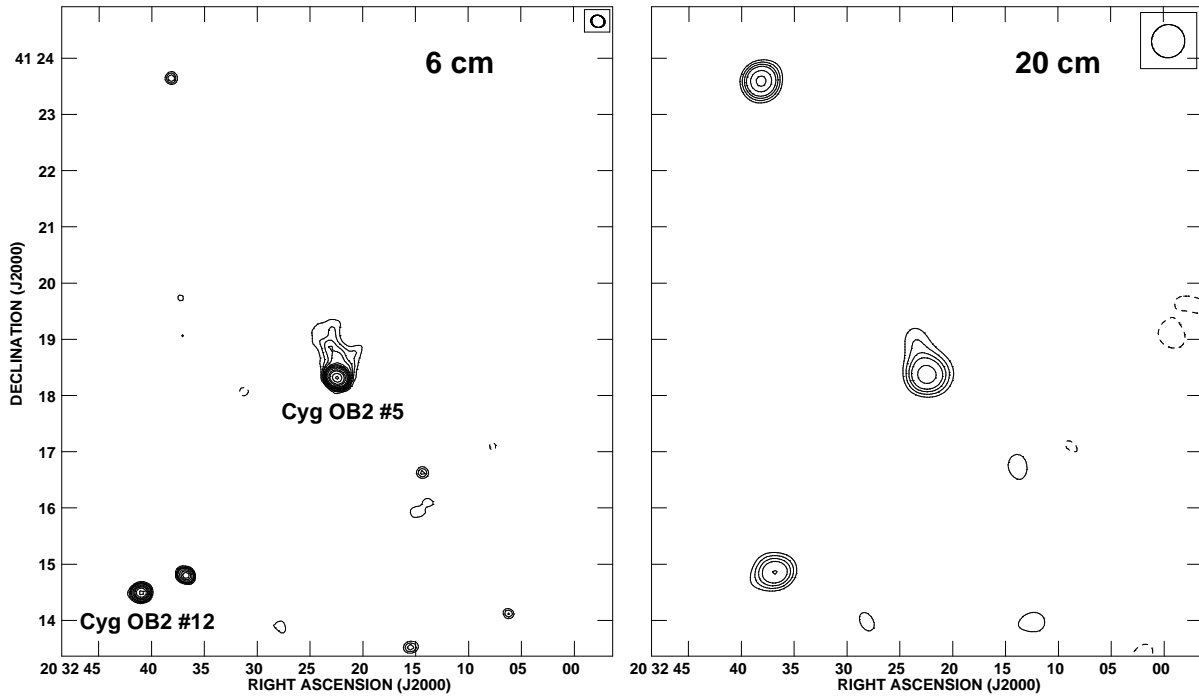


Fig. 2. (Left) A larger VLA contour image of the 6-cm continuum emission toward Cyg OB2 #5. The stars Cyg OB2 #5 and Cyg OB2 #12 are identified. The other radio sources do not have known counterparts. (Right) VLA contour image of the 20-cm continuum emission toward Cyg OB2 #5. Contours are -3, 3, 4, 5, 6, and 8 times $725 \mu\text{Jy}$, the rms noise of the image. The synthesized beam, shown in the top right corner, has half power full width dimensions of $35''8 \times 35''1$, with the major axis at a position angle of -44° . These images are not corrected for the primary beam response. Several of the sources detected in the 6 cm image, including Cyg OB2 #12, are not detected in the 20 cm image given the much larger noise of the latter.

1 k λ . The 20 cm data are difficult to use because of contamination from extended emission, and the field contains other features of strength comparable to that proposed to be associated with Cyg OB2 #5. However, we believe the reality of the NE feature because it is present at both wavelengths.

3. INTERPRETATION

In order to investigate the character of the extended emission, we determined the spectral index of the bright source and the faint component from the 6 and 20-cm data. The 6-cm data was degraded in angular resolution to match that of the 20-cm data. In Figure 3 we show images of radio continuum at 6 and 20 cm in the upper and middle panels, respectively. A spectral index map was made with these images using the AIPS task COMB and it is shown at the bottom panel of Figure 3.

From analysis of the images shown in Figure 3, we determine for the bright compact component a flux density of 7.9 ± 0.2 mJy at 6 cm and 6.8 ± 0.4 mJy at 20 cm. For the extended emission we determine a flux density of 2.1 ± 0.4 mJy at 6 cm and 4.1 ± 1.0 mJy at 20 cm. The spectral index is 0.12 ± 0.05 for the bright compact component, consistent with the value expected for the high state of the variable flux, while for the extended component this value is -0.6 ± 0.3 , indicating that the faint emission is non-thermal, most likely of a synchrotron nature. The spectral index of the extended component is consistent with the value of -0.5 expected for synchrotron emission from shock accelerated electrons (Jun & Jones 1999). We then propose that the extended emission to the NE of the bright component could be i) an unresolved background source (i. e. a radio galaxy), ii) extended galactic emission, or iii) non-thermal emission of relativistic electrons that are produced in the wind-collision region between the stellar winds from the contact binary and the B-type star and that are carried away to large distances by the wind from the contact binary.

3.1. A Background Source?

Using the formulation of Fomalont et al. (1991) we estimate that the probability of finding a background source with a flux of 2.1 mJy at 6 cm in a $2' \times 2'$ box is only 1.1%. This probability is small, however we cannot rule out the possibility that the extended emission can be a background source projected near of Cyg OB2 #5. An image with better angular resolution than that of Figure 1 could reveal the morphology of a radio galaxy and favor this interpretation. Lacking at present such a radio image, we searched through the available infrared survey-images in order to look for any possible infrared counterpart to the extended non-thermal radio source reported here that may give an indication of its nature.

We analyzed the available 2MASS images in the *JHK* bands as well as those taken by the *Spitzer Space Observatory* at 3.6, 4.5, 5.8 and 8 μ m (IRAC) and at 24 μ m (MIPS). Only unresolved sources were found within or close to the radio contours on all these images. In Figure 4, an identification chart is presented on a 4.5 μ m gray-scale IRAC frame. Aperture photometry with appropriate “sky” subtraction of all sources was performed on the Spitzer images and near-infrared photometric data was retrieved from the 2MASS Point Source Catalogue. When possible, these were supplemented by differential aperture photometry on the *JHK* images for those sources omitted in the published catalog. Nevertheless, diffraction spikes prevented us from obtaining reliable near-infrared photometry for sources D, J and H. The near-infrared photometry of Cyg OB2 #5 is from Torres-Dodgen et al. (1991)

The results are given in Table 2. When the photometric uncertainties were of the order of 10 to 15%, the results are given with one decimal; otherwise, these are around 5%. The data for the bright binary star Cyg OB2 #5 are also included for comparison. From their location on all infrared two-color diagrams, we could assert that sources B, C, E, F and, naturally, Cyg OB2 #5 have 1.2 to 8 μ m colors totally consistent with being reddened mid- to early-spectral type photospheres. Sources A, H and J display 1 to 24 μ m colors consistent with Class II pre-main sequence stars. Sources D and G also show slight infrared excesses. With the probable exception of sources B and E, the characteristics of this small group of infrared point sources is representative of the population of young stellar objects in Cyg OB2 (cf. Hora et al. 2011).

Still, the above exercise does not prove that any of the infrared-excess sources cannot be an active radio galaxy, since some of these may have similar infrared colors (e.g. Donley et al. 2008, Kouzuma & Yamaoaka 2010). Nevertheless, we consider this to be very unlikely, as further supported by the results of the complete Spitzer Legacy Survey of the Cygnus-X region described by Hora et al. (2011). These authors found that the known AGN galaxies detected by IRAC in the region were all fainter than $[4.5] \simeq 14$, and were considerably redder than the sources reported here.

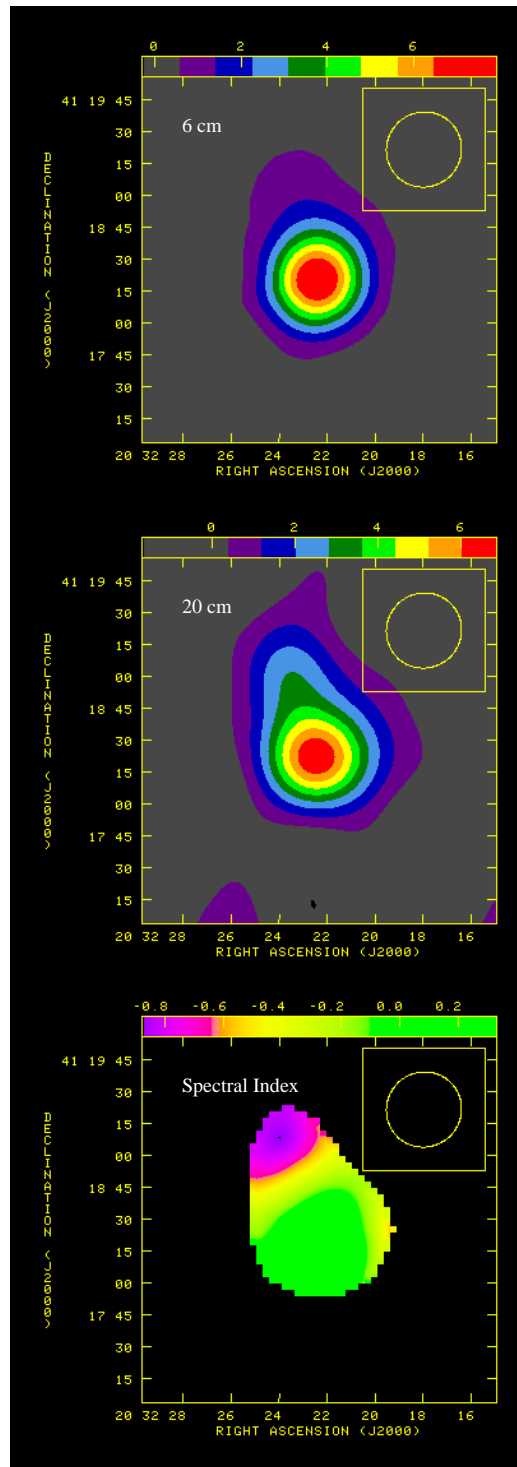


Fig. 3. VLA color images of the 6-cm (top) and 20-cm (middle) continuum emission toward Cyg OB2 #5. The spectral index of the emission is shown in the bottom panel. The flux density and spectral index scales are given in the upper part of the panels. The restoring beam, shown in the top right corner, has half power full width dimensions of $36'' \times 35''$, with the major axis at a position angle of -44° .

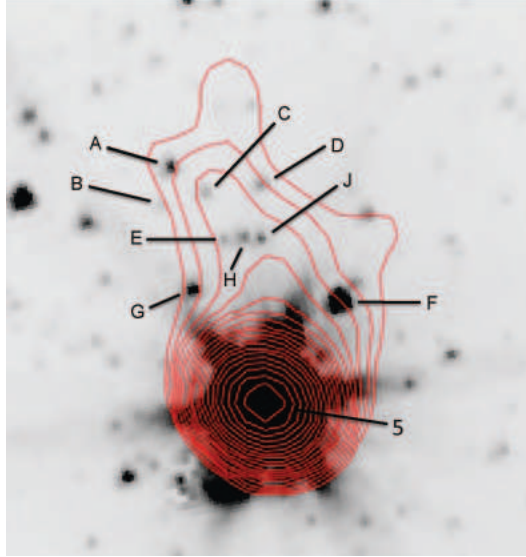


Fig. 4. Identification chart of all point sources listed in Table 2 over an IRAC 4.5 μm image. All sources lie within or close to the (shown) contours of the extended faint 6-cm emission to the north of Cyg OB2 #5. The field of view is 86×93 square arcsecs. North is to the top and east to the left.

TABLE 2

COORDINATES AND IR MAGNITUDES OF SOURCES CLOSE TO THE EXTENDED RADIO SOURCE

| | (J2000) | | <i>J</i> | <i>H</i> | <i>K</i> | [3.6] | [4.5] | [5.8] | [8] |
|---|------------|----------|----------|----------|----------|-------|-------|-------|------|
| A | 20 32 23.8 | 41 18 57 | < 16 | 15.8 | 14.9 | 13.30 | 12.66 | 12.64 | 12.1 |
| B | 20 32 23.9 | 41 18 51 | < 16 | 15.64 | 14.84 | 14.69 | 14.73 | 15.2 | - |
| C | 20 32 23.3 | 41 18 53 | 15.38 | 14.56 | 14.15 | 14.11 | 14.14 | 14.6 | 14.7 |
| D | 20 32 22.5 | 41 18 54 | - | - | - | 13.63 | 13.51 | 14.3 | 14.1 |
| E | 20 32 23.0 | 41 18 45 | 16.1 | 14.62 | 14.15 | 14.0 | 14.2 | 14.7 | - |
| H | 20 32 22.7 | 41 18 46 | - | - | - | 13.5 | 13.3 | 13.7 | 13.2 |
| J | 20 32 22.5 | 41 18 46 | - | - | - | 13.6 | 13.6 | 13.9 | 13.2 |
| G | 20 32 23.5 | 41 18 37 | 15.52 | 14.52 | 13.77 | 12.70 | 12.42 | 12.45 | 12.5 |
| F | 20 32 21.3 | 41 18 35 | 11.39 | 10.94 | 10.67 | 10.83 | 10.80 | 11.07 | 11.4 |
| 5 | 20 32 22.4 | 41 18 19 | 5.24 | 4.55 | 4.27 | 3.5 | 3.6 | 3.7 | 3.8 |

3.2. *Extended Galactic Emission?*

Cyg OB2 #5 is in the local (Cygnus) arm of the Galaxy, very close to the galactic plane and surrounded by complex, extended low surface brightness emission, making this possibility likely. However, the image shown in Figure 2 shows that the only clear extended component is the one associated with Cyg OB2 #5.

3.3. *Relativistic Electrons from the Shock?*

The third possibility for the explanation of the extended emission is interesting because it would imply that small systems of massive stars with non-thermal emission like Cyg OB2 #5 can be sources of relativistic electrons for the interstellar medium. In this explanation the relativistic electrons produced in the interaction between the winds of the contact binary and the B-type stellar companion (that produce the non-thermal NE compact component) could be carried away, together with magnetic fields, by the wind of the contact binary to produce faint, extended non-thermal emission.

We then estimate the minimum energy of the relativistic electrons accelerated in the wind interaction region and the magnetic field that produce the non-thermal secondary component $0''.8$ to the NE of the primary and then ask if these parameters are consistent with the electrons being able to travel to a distance equal to the size of the extended non-thermal emission. This estimate is relevant to check that the relativistic electrons produced in the secondary compact NE region can travel into the interstellar medium and produce the extended component.

Assuming minimum total (magnetic plus relativistic electrons) energy and a homogeneous spherical source, we can use the equations of Pacholczyk (1970) to roughly estimate the magnetic field and the relativistic electron minimum energy in the secondary NE component. In the absence of a detailed knowledge of the nature of the source, these assumptions are consistent with the available data. We adopt a flux of 0.8 mJy at 6 cm for the region (Kennedy et al. 2010) and 1.7 kpc as the distance to the source (Torres-Dodgen et al., 1991). The radius of the emitting region is $\sim 2.5 \times 10^{15}$ cm. We also use 1–30 GHz as the frequency range observed. This gives a magnetic field of 2.0 mGauss and an electron minimum energy of 8×10^{39} ergs.

The Lorentz γ factor for these relativistic electrons is 2×10^3 and the lifetime of them in such a magnetic field is 5×10^3 years (Pacholczyk 1970). Hence, if the electrons are carried away by the wind from the contact binary, whose terminal velocity is adopted to be ~ 2200 km s $^{-1}$ (Bieging et al. 1989), then they can travel emitting centimeter synchrotron radiation up to a distance of ~ 10 pc. This distance corresponds to an angular size of $\sim 20'$ which is much greater than the size of the extended emission, of only $\sim 30''$. However, the post-shock velocity of the wind will be much smaller than the original wind velocity (1/4 for the case of an adiabatic shock) and the distance that the relativistic electrons can travel will be correspondingly smaller ($\sim 5'$) but still much larger than the size of the extended emission ($\sim 30''$). Additionally, the obliquity of the shock geometry can further reduce the post-shock velocity of the wind, but we have a margin of a factor of ~ 10 and conclude that the size of the extended emission detected is not an obstacle for associating it with relativistic electrons produced in the compact secondary NE source. We have also considered the relevance of inverse Compton (IC) cooling. Even when this cooling is more important than synchrotron cooling close to the star, the gas that carries the relativistic electrons is moving away very fast from the star and it can be shown (see Appendix) that IC cooling will not produce a major energy loss.

We now discuss if the electron energy of 8×10^{39} ergs in the secondary NE source can be produced by transforming a fraction of the kinetic energy of the binary wind into the acceleration of the electrons. The secondary NE source subtends a full opening angle of $\sim 30^\circ$, as measured from the primary component and this suggest that it intercepts about 2% of the contact binary wind (see middle panel of Figure 1). Adopting a mass-loss rate of $5 \times 10^{-5} M_\odot$ yr $^{-1}$ (Contreras et al. 1996) and a terminal velocity of 2200 km s $^{-1}$ (Bieging et al. 1989) for the contact binary wind we obtain a total wind kinetic power of 7.8×10^{37} ergs s $^{-1}$. The secondary NE source width (over the line that joins it with the binary) is $\sim 0''.1$. This corresponds to a distance of 2.6×10^{15} cm, that the wind would go over in 1.2×10^7 s (0.4 years). Then, during this time the contact binary wind deposits into the secondary compact NE source an energy of 7.8×10^{37} ergs s $^{-1} \times 1.2 \times 10^7$ s $\times 0.02 = 1.8 \times 10^{43}$ ergs. Therefore, to explain the energy of the relativistic electrons in the secondary compact NE source (8×10^{39} ergs) produced by the shock of the stellar winds from the contact binary and the B-type star, we need an acceleration mechanism that converts 0.04% of the wind's kinetic energy from the contact binary into the acceleration of the relativistic electrons. We note that this relatively low efficiency is consistent with

the results of studies (Eichler & Usov 1993; Ellison & Reynolds 1991; Blandford & Eichler 1987) that indicate that the relativistic electron energy is unlikely to be more than 5% of the total available shock energy, and could conceivably be much less. For the non-thermal extended region we use a flux density of 2.1 mJy at 6 cm and an angular size of $30''$, with the source located at a distance of 1.7 kpc from the Sun. This gives a magnetic field of $\sim 28 \mu\text{Gauss}$ and an electron minimum energy of $\sim 1 \times 10^{43}$ ergs.

An independent consistency check between the synchrotron luminosity and the luminosity of the WCR can be made following Kennedy et al. (2010). For the luminosity of the wind-collision-region we obtain $L_{WCR} \simeq 1.6 \times 10^{36} \text{ erg s}^{-1}$. The radio synchrotron luminosity L_{syn} arising from the WCR, can be estimated from $L_{syn} \simeq 10^{-8} L_{WCR}$ (Chen & White 1994; Pittard & Dougherty 2006), giving an expected synchrotron luminosity from the WCR of $1.6 \times 10^{28} \text{ erg s}^{-1}$. Integrating the radio luminosity in the 1 to 30 GHz range, we obtain a synchrotron luminosity of $5.4 \times 10^{28} \text{ erg s}^{-1}$, that given the uncertainties is consistent with the expected value. The radio luminosity of the extended NE component is about three times larger than that of the compact NE component. Since under our assumptions these radio luminosities are coming from the kinetic power of the wind, this implies that a few more times power is dissipated in the extended component as compared to the compact component.

3.4. Timescale for the acceleration of the relativistic electrons

Finally, we estimate the characteristic timescale for acceleration of the relativistic electrons in the interaction region of the stellar winds from the contact binary and the B-type star, that is, the compact secondary NE source. This is an important estimate to make since, as shown before, the crossing time of the contact binary wind across this region is of only $1.2 \times 10^7 \text{ s}$ (0.4 years). Following Loeb & Waxman (2000), this characteristic timescale, t_{acc} , is given by

$$\left[\frac{t_{acc}}{hr} \right] \sim 1.4 \left[\frac{\gamma}{10^3} \right] \left[\frac{B}{mG} \right]^{-1} \left[\frac{v_{sh}}{10^3 \text{ km s}^{-1}} \right]^{-2},$$

where γ is the Lorentz factor of the relativistic electrons, B is the magnetic field of the region, and v_{sh} is the shock velocity. Adopting $\gamma = 2 \times 10^3$, $B = 2.0 \text{ mGauss}$, and $v_{sh} = 2200 \text{ km s}^{-1}$, we obtain $t_{acc} \sim 0.3$ hours. Then, the acceleration takes place very quickly, on a timescale much shorter than the wind crossing time.

4. CONCLUSIONS

We present the analysis of VLA archive data of the Cyg OB2 #5 system taken during 1984 in the low angular resolution D configuration.

Concatenating 6 and 20-cm data, we detect an extended region of non-thermal emission to the NE of the compact components of Cyg OB2 #5. This faint emission could be an unresolved background source, like a radio galaxy, but photometry performed on archival 2MASS and *Spitzer* images on all infrared sources in the vicinity suggests that this possibility is highly unlikely. It is also possible that the emission is produced by synchrotron radiation of the relativistic electrons produced in the shock of the stellar winds from the contact binary and the B-type star to its NE and carried away at large distances by the stellar wind of the contact binary. However, we cannot rule out the possibility that the emission arises in an extended galactic feature unrelated to the stellar system.

We end by noting that Cyg OB2 #5 is a remarkable system in that it shows radio structures over different scales, from about 10 milliarcseconds to about 30 arcseconds, a range of 3×10^3 (see Fig. 1). At the 10 milliarcsecond scale, Ortiz-León et al. (2011) have used Very Long Baseline Array observations to detect the non-thermal, arc-like structure that traces the wind-collision region between the wind of the contact binary and that of an unseen nearby companion. At the scale of $\sim 0''.1$, one can detect the thermal (free-free) emission from the wind of the contact binary (Rodríguez et al. 2010). About $1''$ to the NE of the contact binary, one finds the nonthermal compact NE component (Contreras et al. 1999) that results from the interaction of the winds of the contact binary and that of a known B-type star (Herbig 1967). Finally, in this paper we propose that an extended ($\sim 30''$) structure detected to the NE could also be associated with this multiple stellar system.

We thank an anonymous referee for suggestions that greatly improved our original Figures 1 and 2. GNOL and LFR are thankful for the support of DGAPA, UNAM, and of CONACyT (México). MT acknowledges

DGAPA/PAPIIT grant No. 100210. This research has made use of the SIMBAD database, operated at CDS, Strasbourg, France. This work makes use of archival data obtained with the Spitzer Space Telescope, which is operated by the Jet Propulsion Laboratory, California Institute of Technology under a contract with NASA. Support for this work was provided by an award issued by JPL/Caltech. Also of data products from the Two Micron All Sky Survey, which is a joint project of the University of Massachusetts and the Infrared Processing and Analysis Center/California Institute of Technology, funded by the National Aeronautics and Space Administration and the National Science Foundation.

APPENDIX

A. INVERSE COMPTON COOLING IN GAS MOVING AWAY FROM A STAR

The rate of inverse Compton energy loss of a relativistic electron at a distance r_0 of a star with luminosity L is given by (Pittard et al. 2006):

$$\frac{d\gamma}{dt} = -\frac{\sigma_T \gamma^2 L}{3\pi m_e c^2 r_0^2},$$

where γ is the Lorentz factor of the electron, σ_T is the Thomson cross section, m_e is the electron mass, and c is the speed of light.

Integrating this equation, we find that the timescale for a relativistic electron to lose one half of its initial energy is given by

$$t_S = \frac{3\pi m_e c^2 r_0^2}{\gamma_0 \sigma_T L}.$$

However, in the scenario discussed in the paper, the gas is rapidly moving away from the star. In this case, the energy loss equation can be put as:

$$\frac{d\gamma}{dt} = -\frac{\sigma_T \gamma^2 L}{3\pi m_e c^2 r^2},$$

where the radius r is increasing with time and is given by $r = r_0 + vt$, where r_0 is the initial radius considered and v is the wind velocity. On the other hand, the crossing time of the gas from the star to the shock region is given by $t_C = r_0/v$.

Solving the previous equation it can be found that for the relativistic electron to reach infinity without having lost one half of its energy the following condition should be fulfilled:

$$t_C \leq t_S,$$

while for this loss to take place in finite distances we need

$$t_C > t_S.$$

In the case discussed in the paper, we have $\gamma_0 = 2 \times 10^3$, $r_0 = 2.0 \times 10^{16}$ cm, $L = 10^6 L_\odot$ (Linder et al. 2009) and $v = 2200$ km s⁻¹. However, the luminosity of Linder et al. (2009) was estimated for a distance of 925 pc. Correcting for the distance of 1.7 kpc used in our other estimates, we obtain $L = 3 \times 10^6 L_\odot$. We then obtain $t_S \simeq 6$ yr and $t_C \simeq 3$ yr. We are then in the case $t_C \leq t_S$ and inverse Compton scattering produced by the radiation field of the contact binary is not expected to dominate the energy loss.

The B-type star to the NE of the contact binary will have a much smaller luminosity but it will produce important inverse Compton losses to the relativistic electrons that pass very close to it. To estimate its effect on the bulk of the relativistic electrons, we note that the angular radius of the compact NE source (2.5×10^{15} cm) is about an order of magnitude smaller than the distance between the contact binary and the NE compact source (2.0×10^{16} cm). We also note that its approximate spectral type (B0 V-B2 V) was derived by Contreras et al. (1997) from Hipparcos photometry. Adopting the mean spectral type of B1 V, we estimate a bolometric luminosity of $L \simeq 10^4 L_\odot$ (Panagia 1973), about 300 times less than that of the contact binary. Since the effect of the inverse Compton scattering goes as luminosity over distance squared, we conclude that, on the bulk, the effect of the B-type star will be a few times smaller than that of the contact binary.

REFERENCES

- Abbott, D. C., Biegging, J. H., & Churchwell, E. 1981, *ApJ*, 250, 645
- Biegging, J. H., Abbott, D. C., & Churchwell, E. B. 1989, *ApJ*, 340, 518
- Blandford, R., & Eichler, D. 1987, *Phys. Rep.*, 154, 1
- Briggs, D. 1995, Ph.D. thesis, New Mexico Inst. of Mining and Technology
- Chen, W., & White, R. L. 1994, *Ap&SS*, 221, 259
- Contreras, M. E., Rodríguez, L. F., Gómez, Y., & Velázquez, A. 1996, *ApJ*, 469, 329
- Contreras, M. E., Rodríguez, L. F., Tapia, M., Cardini, D., Emanuele, A., Badiali, M., & Persi, P. 1997, *ApJ*, 488, L153
- Donley, J. L., Rieke, G. H. Pérez-González, P. G., & Barro, G., 2008, *ApJ* 687, 111
- Eichler, D., & Usov, V. 1993, *ApJ*, 402, 271
- Ellison, D. C., & Reynolds, S. P. 1991, *ApJ*, 382, 242
- Fomalont, E. B., Windhorst, R. A., Kristian, J. A., & Kellerman, K. I. 1991, *AJ.*, 102, 1258
- Hall, D. S. 1974, *Acta Astronomica*, 24, 69
- Herbig, G. H. 1967, *PASP*, 79, 502
- Hora, J. L., et al. 2011, in *Reionization to Exoplanets: Spitzer Growing Legacy*, ed. P. Ogle, ASPCS (in press)
- Jun, B.-I., & Jones, T. W. 1999, *ApJ*, 511, 774
- Kennedy, M., Dougherty, S. M., Fink, A., & Williams, P. M. 2010, *ApJ*, 709, 632
- Kozouma, S., & Yamaoaka, H., 2010, *A&A* 509, A64
- Leung, K.-C., & Schneider, D. P. 1978, *ApJ*, 224, 565
- Linder, N., Rauw, G., Manfroid, J., Damerdj, Y., De Becker, M., Eenens, P., Royer, P., & Vreux, J.-M. 2009, *A&A*, 495, 231
- Loeb, A., & Waxman, E. 2000, *Nature*, 405, 156
- Miralles, M. P., Rodríguez, L. F., Tapia, M., Roth, M., Persi, P., Ferrari-Toniolo, M., & Curiel, S. 1994, *A&A*, 282, 547
- Ortiz-León, G. N., Loinard, L., Rodríguez, L. F., Mioduszewski, A. J., & Dzib, S. A. 2011, *ApJ*, 737, 30
- Pacholczyk, A. G. 1970, *Series of Books in Astronomy and Astrophysics*, San Francisco: Freeman
- Panagia, N. 1973, *AJ*, 78, 929
- Persi, P., Ferrari-Toniolo, M., Tapia, M., Roth, M., & Rodríguez, L. F. 1985, *A&A*, 142, 263
- Persi, P., Tapia, M., Rodríguez, L. F., Ferrari-Toniolo, M., & Roth, M. 1990, *A&A*, 240, 93
- Pittard, J. M., Dougherty, S. M., Coker, R. F., O'Connor, E., & Bolingbroke, N. J. 2006, *A&A*, 446, 1001
- Rauw, G., Vreux, J.-M., & Bohannan, B. 1999, *ApJ*, 517, 416
- Rodríguez, L. F., Gómez, Y., Loinard, L., & Mioduszewski, A. J. 2010, *RMxAA*, 46, 215
- Torres-Dodgen, A. V., Tapia, M., & Carroll, M. 1991, *MNRAS*, 249, 1

Gisela N. Ortiz-León and Luis F. Rodríguez: Centro de Radioastronomía y Astrofísica, UNAM, A. P. 3-72, (Xangari), 58089 Morelia, Michoacán, México (g.ortiz, l.rodriguez@crya.unam.mx).

Mauricio Tapia: Instituto de Astronomía, Universidad Nacional Autónoma de México, Apartado Postal 877, Ensenada, Baja California, CP 22830, México (mt@astrosen.unam.mx).